J. COMBIN. MATH. COMBIN. COMPUT. 127b (2025) 1643--1658

Journal of Combinatorial Mathematics
and Combinatorial Computing
www.combinatorialpress.com/jcmcc

Combinatorial Press

Research on the application of artificial intelligence in coal mine gas monitoring and prediction

Jie Zhang[1,2,✉]

[1] Department of Management Information, Anhui College of Mining and Technology, Huaibei, Anhui, 235000, China

[2] Department of Management Information, Huaibei Coal Technicians College of Anhui, Huaibei, Anhui, 235000, China

ABSTRACT

This study investigates the application of artificial intelligence techniques in coal mine gas monitoring and prediction, aiming to construct more efficient and accurate gas concentration prediction models to reduce the risk of gas explosion in coal mine production. Due to the limited performance of traditional prediction methods in dealing with high-dimensional and dynamic three-dimensional mining environments, this study employs a fusion model based on temporal convolutional network (TCN) and temporal generative adversarial network (TimeGAN), TCN-TimeGAN, to predict the gas concentration. The model combines the interval sampling advantage of TCN and the time series characteristics of TimeGAN, and through four processes of embedding, recovering, by generating and discriminating gas concentration time sequences, the time-dependent features of gas concentration data can be effectively captured, thus improving the prediction accuracy and timeliness. In this study, gas concentration data from September 2020 through December 2021 were used as the basis, through data cleaning and outlier processing, it is found that the gas concentration data has obvious time-dependence, which is suitable for using time series modeling. Embedding and Recovery Networks via TCN-TimeGAN Modeling, the gas concentration data are mapped to a low-dimensional feature space, a generative network is then used to generate new time series data from random noise, and the model parameters are optimized by combining the discriminative network in order to improve the quality and consistency of the generated data. In particular, to cope with the problem of gradient instability of generative adversarial networks during training, In this paper, Wasserstein distance is introduced to optimize the loss function and a gradient penalty term is added during the training process to improve the stability of model training and the realism in the samples generated. In addition, this study also explores the prediction performance of combining LSTM networks for gas concentration. The standard recurrent neural network (RNN) faces the problem of gradient vanishing in the processing of long time-dependent data, whereas the improved LSTM overcomes this problem through memory cells and gating mechanism for real-time prediction task of gas concentration. In this study, the LSTM is further extended to three-dimensional spatial input data, experiments demonstrate the prediction accuracy

✉ Corresponding author.
E-mail address: flu0626@163.com (J. Zhang).

Received 20 July 2024; Revised 10 October 2024; Accepted 05 February 2025; Published Online 16 April 2025.
DOI: 10.61091/jcmcc127b-091

of the improved LSTM. To verify the validity of the model, this paper adopts a hierarchical K-fold cross-validation method, which divides the data into a training set and a validation set to ensure that the model can be generalized. Experimental results indicate that TCN-TimeGAN and improved LSTM significantly outperform traditional methods in gas concentration prediction. By analyzing the training and validation accuracies, the models showed high prediction accuracy (89.1% to 93.8%) after 20 epochs, verifying the stability and applicability of the models.

In conclusion, this study shows that the gas prediction model based on TCN-TimeGAN and improved LSTM can more accurately predict the gas concentration in coal mines, improve the intelligence level of coal mine gas monitoring, and provide technical support for safe production in coal mines. Meanwhile, the methods and models in this study also provide new thoughts and methods for time series data prediction in other fields.

Keywords: Coal Mine Gas Monitoring, TCN-TimeGAN, Gas Concentration Prediction, LSTM Network, Deep Learning

1. Introduction

Energy is an important driving force to support the sustainable development of society, and in the process of China's economic and social development, coal resources are the main source of energy for development [1]. After entering the new period of industrialized production, with the effective supervision of the relevant state departments and the application of high-tech products in coal mines, the conditions of coal mine safety production have been upgraded, and the level of safety production in the coal mining industry has been improved to some extent [2-4]. However, due to the complex geological conditions underground in coal mines and the sudden uncontrollable factors in the process of coal mining, coal mine safety accidents occur from time to time. Gas accidents are an important problem facing the healthy and sustainable safety production of China's coal industry [5]. Safe underground coal mine operation is an important guarantee for the sustainable development of coal mining enterprises and the life safety of coal miners, which is related to the development of China's energy industry and economic and social development [6-7]. Ensuring safe production in coal mines, fully recognizing the importance and urgency of gas prevention and control, adhering to the "safety first" principle, improving the management level, and reducing the occurrence of accidents are the ongoing concerns of the coal mining industry [8-10].

In order to effectively reduce the incidence of coal mine gas accidents, coal mining enterprises will apply high-tech products to coal mine safety production, coal mine underground mining equipment, ventilation technology and personnel management level has been greatly improved, mining technology to further improve the prevention of gas accidents has become an important guarantee of coal mine safety production [11-14]. The traditional method of gas detection in underground coal mines mainly consists of installing sensors at fixed locations for spot monitoring and arranging coal mine gas inspectors for patrol monitoring [15-17]. Although it solves the problem of coal mine gas monitoring to a certain extent, there are many shortcomings such as low coverage, poor monitoring accuracy, high work intensity, large safety risks, and it is impossible to achieve real-time gas disaster warning [18-20]. The integration of artificial intelligence technology in coal mine gas intelligent monitoring system can use the Internet communication technology to transmit the data of gas, wind speed, temperature, etc. from each measurement point to the ground computer storage system, so that the gas, wind speed, temperature, etc. in each key area of the coal mine underground have been effectively monitored in real time and alarmed for exceeding the limit [21-24]. To a great extent, it promotes the development of the field of intelligent monitoring of coal mine gas, so that the coal mine engineering practitioners can obtain the time-varying information of gas concentration in a timely manner.

2. Gas Intelligent Prediction Model Construction

In dynamic environments such as longwall mining, where continuous monitoring is essential to prevent explosion hazards, relying solely on advance prediction is not sufficient to achieve the objectives of this study. Moreover, it is not realistic to implement these prediction methods in real time considering the required computational resources and data size. Due to the three-dimensional geometry of longwall mining, these statistical methods do not predict well in a three-dimensional environment. Moreover, statistical methods rely on interpolation and cannot learn extreme fluctuations in data as artificial intelligence models do. Therefore, in this study, advanced artificial intelligence algorithms will be used to monitor and predict gas concentrations.

2.1. Analysis of gas concentration data

The processed gas concentration data demonstrates its time series properties, which are the basis for modelling and prediction of gas concentrations. Therefore, this paper begins with a detailed analysis of these temporal properties. In this study, gas data from the 15103 working face of a mine was selected for the study., and the data were collected and recorded every 24 hours. In the process of data collation, it was found that there existed periodic salient points with excessive concentration, which were usually due to the alarm value during equipment tuning or inspection and testing, and belonged to the artificially increased value. For these anomalous points, we used the method of mean value interpolation for processing, and the processed results for Figure 1.

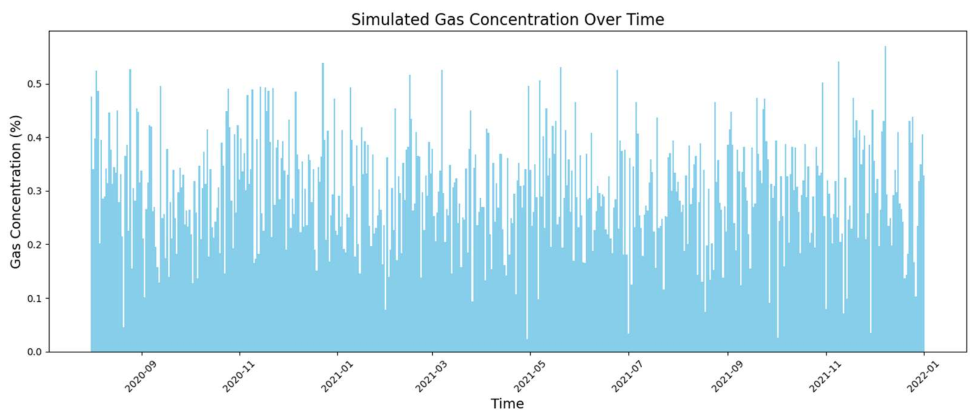

Fig. 1. Graph of data processing results

In addition, gas data views at one point in time are closely related to those at the previous point in time or even to multiple points in time, showing obvious time-dependent characteristics. Therefore, such data characteristics are very suitable for modelling using TimeGAN network. Considering the advantages of the TCN network in handling interval sampling data, the TCN-TimeGAN model, which combines TCN and TimeGAN, is chosen for predictive modelling of gas data in this paper.

Next, we describe in detail the process of constructing and applying the TCN-TimeGAN model and demonstrate its effectiveness in gas data prediction.

2.2. TCN-TimeGAN Infrastructure Network

Traditional convolutional neural networks, when dealing with long time series data, linearly stack hidden layers due to the need to trace back too much historical information, resulting in the network becoming extremely deep, which in turn increases the difficulty of processing. TCN (Temporal Convolutional Networks) solves this problem by employing the inflated causal convolution, which employs spaced samples rather than one-by-one samples in performing convolutional calculations, thus reducing the number of convolutional layers, while at the same time, it reduces the number of convolutional layers without loss of information, a larger receptive field is obtained and features of longer time dimension can be read more efficiently. Therefore, by combining the interval sampling advantage of TCN and the time series feature of TimeGAN, TCN-TimeGAN shows significant advantages in processing gas data.

The TCN-TimeGAN network consists of four components: embedding (E), recovery (R), generation (G) and discriminative network (D). First, the embedding and recovery network maps the database into a lower dimensional dimension to capture key features. Given the original time series data $X=\{x_1,x_2,\ldots,x_T\}$ the embedding network E maps it into a low dimensional representation H. The embedding network E maps the data into a low dimensional representation H:

$$H=E(X) \tag{1}$$

Next, the recovery network R decodes the low-dimensional representation H into reconstructed time series data $\hat{X}$.

$$\hat{X}=R(H) \tag{2}$$

To ensure that the key features of the data are maintained, the optimisation process is carried out by minimising the reconstruction loss $\mathrm{L}_{\mathrm{rec}}$ between the original data X and the reconstructed data $\hat{X}$.

$$\mathrm{L}_{\mathrm{rec}}=\mathrm{E}\left[\| X-\hat{X}\|^2\right] \tag{3}$$

The generative network generates new time series data by accepting as input a random noise $Z=\{z_1,z_2,\ldots,z_T\}$,and a conditional vector $C=\{c_1,c_2,\ldots,c_T\}$. $\tilde{X}$.

$$\tilde{X}=G(Z,C) \tag{4}$$

The responsibility of the discriminant net is to recognize resemblance between the real data X and the generation data $\tilde{X}$:

$$\mathrm{L}_{\mathrm{adv}}=\mathrm{E}[\log D(X)]+\mathrm{E}[\log(1-D(\tilde{X}))] \tag{5}$$

In addition, the supervisory network is also used to evaluate the differences in the distributions of feature dimensions and time dimensions between the produced data and the true data within the time window, thus making the produced data more realistic. Supervised loss is:

$$\mathrm{L}_{\mathrm{sup}}=\mathrm{E}\left[\| H-\tilde{H}\|^2\right] \tag{6}$$

where $\tilde{H}=E(\tilde{X})$ is the embedded representation of the generated data.

TCN-TimeGAN combines reconstruction loss, adversarial loss, and supervisory loss by minimizing the total loss function LTCN-TimeGAN $\mathrm{L}_{\mathrm{TCN\text{-}TimeGAN}}$, to improve the quality and consistency of the data generated:

$$\mathrm{L}_{\mathrm{TCN\text{-}TimeGAN}}=\alpha\mathrm{L}_{\mathrm{rec}}+\beta\mathrm{L}_{\mathrm{adv}}+\gamma\mathrm{L}_{\mathrm{sup}} \tag{7}$$

where α , β , and γ are weight hyperparameters. TCN-TimeGAN combines the unsupervised training of GAN with the supervised training of regression model, It captures not only the distribution of features at each point in time, but also the dynamics of these variables over time, thus realizing the enhancement and accurate prediction of time series data.

2.3. TCN-TimeGAN-based gas prediction modeling

In this section, a natural gas power generation forecasting model will be designed on the basis of TCN-TimeGAN base network. Firstly, the gas time series are processed with normalization and missing data values, and the result is used as the input sequence $x=\{x_1,\ldots,x_t,\ldots,x_T\}$ of the model, it is then fed into the insertion network and resumption network for training, with the goal of reducing the reconstruction loss. Here, TCN networks are used to embed networks and restore networks. The embedding network maps the input data x into the low-dimensional feature space, denoted as $\mathrm{H}=\mathrm{E}(\mathrm{x})$, while the recovery network decodes the low-dimensional features H back to the original data space to obtain the reconstructed data $\hat{x}=R(H)$. The model is optimized by minimizing the reconstruction loss $\mathrm{L}_{\mathrm{rec}}=\mathrm{E}\left[\| x-\hat{x}\|^2\right]$ during training.

Next, the input sequence x is fed into the supervised network for training with the goal of reducing the supervisory loss. A supervisor is introduced in the training phase of the supervised network which uses LSTM networks and is primarily used to evaluate the difference of data generated by the generative network from the real data to make the generated data more compliant. The supervisory loss of the supervised network is obtained by calculating the Mean Square Error (MSE) of the output $\tilde{H}$ of the supervisor and the output H of the embedded network:

$$\mathrm{L}_{\mathrm{sup}}=\mathrm{E}\left[\| H-\tilde{H}\|^2\right] \tag{8}$$

The last stage is the joint training process, where the total loss is the total of the generative network loss and the discriminative network loss. There are two main steps in joint training: 1) In each iteration, the generative network is trained with the goal of minimizing the generative network loss L_G, and the generated data $\tilde{x}=\mathrm{G}(z, \mathrm{C})$ is as near as practicable to the real data x. 2) The goal of the discriminative network is to maximize the discriminative network loss L_D, and to improve its ability to discriminate between the real data x and the generated data $\tilde{x}$. The discriminative network loss is defined as:

$$\mathrm{L}_{\mathrm{adv}}=\mathrm{E}[\log D(x)]+\mathrm{E}[\log(1-D(\tilde{x}))] \tag{9}$$

The TCN-TimeGAN network is used for the prediction of gas density and its training process includes the following three main functions:

Feature vector encoding: the incoming data is coded by embedding the network E in order to extract the key feature representations H. The feature vectors are encoded by embedding the network E in order to extract the key features.

Potential Distribution Representation: The generative network G ensures that the generated data conforms to the true data distribution by generating the data $\tilde{x}=G(z,C)$ from the random noise z.

Iteration in the time dimension: Capture the dynamics of the data in the time dimension through multiple iterations of optimization.

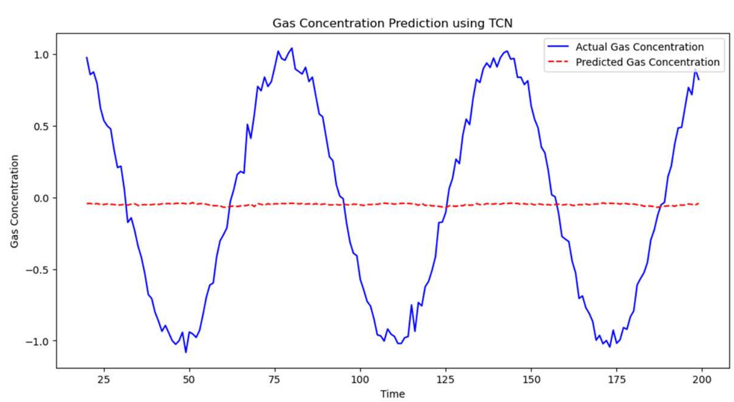

Fig. 2. Comparison of predicted gas concentrations

After the completion of these three stages of training, a network model and its parameters that can be used for gas prediction are obtained. For gas prediction, random sequences are regenerated and input into the trained gas prediction model to get the target generation data. The target-created data and the true data are fed into the prediction model as training and test sets, respectively, respectively, and through several iterations of optimization, the final prediction results are obtained as shown in Figure 2.

3. Predictive Model Loss Function

TCN-TimeGAN and GAN networks usually face the problems of gradient instability, pattern collapse, and training difficulty. To deal with these deficiencies, this paper presents the Wasserstein loss, which optimizes the loss factor of the discriminative net, thus effectively alleviating these training bottlenecks.

3.1. Improved loss function based on Wasserstein distance

In generation and discrimination nets, KL dispersion is often employed to measure the difference in spread between real and generative data. Assuming that p represents the true sample distribution and q indicates the generated sample distribution, then as q gets closer to p, the smaller the value of the dispersion and the smaller the loss. However, there are two problems in the application of KL dispersion:

The KL dispersion is asymmetric, i.e. $D_{KL}(p \parallel q) \neq D_{KL}(q \parallel p)$. This means that different results are obtained when p and q are exchanged, which creates difficulties when comparing and interpreting differences between distributions.

KL dispersion is too sensitive to noise or outliers to be used for unbalanced timing data.

While the JS scattering (Jensen-Shannon scattering) solves the asymmetry problem of the KL scattering, in the case of incomplete overlap of the distributions, the value of the JS scattering becomes a constant $\log 2$, which means that the gradient is zero at this point, i.e., the gradient vanishes. This situation is very detrimental in learning algorithms because the lack of gradient leads to training stagnation and the inability to continue optimizing the model.

In contrast, the Wasserstein distance still reflects the distance between two distributions when they do not overlap, and even in cases where the KL and JS dispersions do not provide a gradient, the Wasserstein distance still provides a meaningful gradient, ensuring effective learning of the generative model.

Wasserstein range is defined as follows:

$$W\left(P_r, P_g\right) = \inf_{\gamma\sim\Pi\left(P_r, P_g\right)} E_{(x,y)\sim\gamma}[\| x-y \|] \tag{10}$$

For each possible joint distribution γ, one can sample a true sample x and a generated sample y from it and compute the distance $|x-y|$ between the pair of samples and its mathematical expectation $E_{(x,y)\sim\nu}[|x-y|]$. The expected value is the lower bound of this expected value in all possibly joint distributed:

$$\inf_{\nu\in M\left(P_r, P_g\right)} E_{(x,y)\sim\nu}[\| x-y \|] \tag{11}$$

Definition of the Wasserstein distance, where $M(P_r, P_g)$ is the set of all possibly joint data distributed between the actual data distributed P_r and the resulting data distribution P_g. The Wasserstein range is a measure of the separation between two distributions. This metric effectively measures the distance between the two distributions, and the Wasserstein distance provides a stable and meaningful gradient during the training process, which helps in the optimization and convergence of the generative model.

In the base network TCN-TimeGAN, the objective functions of the embedding and recovery networks are:

$$\min_{\theta_\theta, \theta_r}\left(\lambda L_S + L_R\right) \tag{12}$$

where y_{real} is the scaling factor, and y_{real} and y_{real} are the supervised and reconstructed loss functions, respectively, defined as:

$$L_S = E_{x_i \sim p(x_t)}\left[\left\|\mathbf{x}_{\mathrm{T}} - G\left(\mathbf{x}_{\mathrm{I\,T-1}}\right)\right\|_{\mathrm{L}}\right] \tag{13}$$

$$L_{\mathrm{R}} = E_{x_{x_i} \sim p(x_t)}\left[\left\|\mathbf{x}_{1:\mathrm{T}} - \mathbf{x}_{1:\mathrm{T}}\right\|_2\right] \tag{14}$$

Where x_t denotes the sample of the $p(x_t)$ moment in the real distribution t, x_{ir} denotes the sample of the first T moments in the real data, and x_{ir} also denotes the sample of the first T moments in the original data. The fusion of these two networks effectively reduces the training complexity of the generative network and significantly improves the authenticity and reliability of the generated data, thus improving the overall performance of the generative network.

The objective functions of the generative and discriminative networks are:

$$\min_{\theta_g}\left(\eta L_S + \max_{\theta_d} L_U\right) \tag{15}$$

where y_{real} is the scaling factor and y_{real} is the generation against loss, defined as:

$$L_U = E_{x_{x_1} \sim p(x_1)}\left[\log D\left(x_{1:\mathrm{T}}\right)\right] + E_{z_{z_t} \sim p(z_t)}\left[\log\left(1 - D\left(G\left(z_{1:\mathrm{T}}\right)\right)\right)\right] \tag{16}$$

where z_t denotes the sample at moment $p(z_t)$ in the random data distribution t, z_1 denotes the sample at the previous moment T in the random data, $G(\cdot)$ denotes the output of the generative network, and $D(\cdot)$ denotes the output of the discriminative network.

The reconstruction loss and the supervised loss reflect the transformation difference of the data in different dimensions, mainly focus on the characteristics of the data itself, and usually use the root mean square error (RMSE) as the loss function. However, Eq. (16) shows that the generative adversarial loss consists of the generative network loss and the discriminative network loss, where the goal of the generative network is to minimize the distribution distance between the generated vectors and the true vectors. Since the Wasserstein distance is more stable in measuring the difference between distributions, it is more suitable for such tasks to optimize the performance of the generative network:

$$G_{\mathrm{Loss}} = W\left(\mathbf{x}, \mathbf{x}_{syn}\right) \tag{17}$$

Where, x denotes the real data and x_{syn} denotes the generated data, which contains the reconstruction loss and the supervision loss.

For a discriminative network, the goal is to maximize the distribution distance between the generated vectors and the true vectors. This goal can be expressed using the Wasserstein distance of the form:

$$W\left(p_r, p_g\right) = \inf_{\gamma \in M\left(p_r, p_g\right)} \mathrm{E}_{(x,\hat{x})\sim\gamma}[\| x - \hat{x} \|] \tag{18}$$

where p_r denotes the distribution of the real data, p_g denotes the distribution of the generated data, γ denotes all possible joint distributions, and $|\cdot|$ is the distance measure between samples. By maximizing the Wasserstein distance, the discriminative network can effectively drive the generative network to generate more realistic and diverse data.

3.2. Improved loss function based on gradient penalty term

TimeGAN may suffer from problems such as gradient vanishing and pattern collapse during the training process. To solve these problems, this paper improves the loss function by introducing the Wasserstein distance, which effectively alleviates these problems. Further, in order to improve the stability of training and the quality of generated samples, this paper adopts the gradient penalty method to constrain the gradient of the discriminative network.

Specifically, the main idea of the gradient penalty is to impose a Lipschitz constraint on the distribution region of the generated and real samples to ensure that the gradient of the discriminative network does not exceed a finite constant K . This constraint helps prevent the network from experiencing gradient explosion or gradient vanishing during the training process, which in turn improves the stability of the training process and enhances the quality of the generated samples.

The implementation of the gradient penalty is usually done by adding a regular term to the optimization process, and the specific loss function can be expressed as follows:

$$L_{\mathrm{WGAN-GP}} = L_{\mathrm{WGAN}} + \lambda \mathrm{E}_{\hat{x}\sim\hat{P}}\left[\left(\left\|\nabla_{\hat{x}} D(\hat{x})\right\|_2 - 1\right)^2\right] \tag{19}$$

where L_{WGAN} is the standard Wasserstein loss, $\hat{x}$ is the sample generated by interpolating between the real and generated data, $\nabla_{\hat{x}} D(\hat{x})$ is the gradient of the discriminative network D over the interpolated sample $\hat{x}$, and λ is a hyperparameter that weighs the gradient penalty term, which is usually taken as a small constant. This term enforces that the gradient of the discriminative network is consistent within the interpolated sample region, which further improves the training effect of the generative model.

Specifically, it is first necessary to sample the real data and generated data, let $x_r \sim P_r$, $x_g \sim P_g$,where P_r denotes the real data distribution and P_g denotes the generated data distribution. Then, take a random interpolation sample between these two, denoted as:

$$\hat{x} = \epsilon x_r + (1-\epsilon) x_g, \quad \epsilon \sim \mathrm{U}(0,1) \tag{20}$$

where $\hat{x}$ is a sample obtained by linearly interpolating x_r and x_g, and ϵ is a random variable sampled from a uniform distribution $\mathrm{U}(0,1)$ to control the proportion of interpolation.

This interpolated sample $\hat{x}$ is used to penalize the gradient of the discriminative network during training to ensure that it meets the Lipschitz continuity requirements and avoids gradient explosion or gradient vanishing. This approach helps stabilize the training and improves the quality of the generated data.

Let the distribution of the interpolated sample $\hat{x}$ be $P_{\hat{x}}$, then the gradient penalty term of the discriminative network can be expressed as:

$$L_{\mathrm{GP}} = \mathrm{E}_{\hat{x}\sim P_{\hat{x}}}\left[\left(\left\|\nabla_{\hat{x}} D(\hat{x})\right\|_2 - 1\right)^2\right] \tag{21}$$

where $D(\hat{x})$ is the output of the discriminative network, $\nabla_{\hat{x}} D(\hat{x})$ denotes the gradient of the discriminative network on the interpolated sample $\hat{x}$, and $|\cdot|_2$ is the L2 norm, which denotes the magnitude of the gradient.

This gradient penalty term serves to penalize regions with gradients exceeding 1, forcing the gradient of the discriminative network to be close to 1 in the interpolated sample space, thus satisfying the Lipschitz continuity constraint. In this way, the phenomenon of gradient explosion or gradient vanishing can be prevented, further improving the stability of the model and the quality of the generated data.

Introducing the gradient penalty term into the above equation yields the improved loss function formula for the discriminative network:

$$L_{\mathrm{D}} = -\mathrm{E}_{x_r\sim P_r}\left[D\left(x_r\right)\right] + \mathrm{E}_{x_g\sim P_g}\left[D\left(x_g\right)\right] + \lambda \mathrm{E}_{\hat{x}\sim P_x}\left[\left(\left\|\nabla_{\hat{x}} D(\hat{x})\right\|_2 - 1\right)^2\right] \tag{22}$$

Among them:

Item I $-\mathrm{E}_{x_r\sim P_r}[D(x_r)]$ is a loss of real data;

The second term $\mathrm{E}_{x_g\sim P_g}[D(x_g)]$ is the loss to the generated data;

The third term is the gradient penalty term, λ is the weight coefficient of the penalty term, $\hat{x} = \epsilon x_r + (1-\epsilon)x_g$ denotes the samples obtained from linear interpolation between real and generated data, and $\nabla_{\hat{x}} D(\hat{x})$ is the gradient of the discriminative network over the interpolated samples.

By introducing a gradient penalty term, the improved loss function of the discriminative network ensures that the gradient of the discriminative network satisfies the Lipschitz continuity, which enhances the stability of training, avoids the gradient explosion or gradient vanishing problem, and improves the quality of the generated data.

The weight factor λ in Eq. (10) has an important impact on the training effect. Some literature proposes to use fixed weights to control the impact of the gradient penalty term, however, this strategy of fixed weights has certain problems in the training process. Specifically, in the early stage of training, too heavy gradient penalty will limit the learning space of the generative network, resulting in the generative network being difficult to learn effectively, which in turn affects the convergence of the model; while in the late stage of training, the fixed penalty weights may not be able to provide sufficient constraints for the generative network, which results in the decrease in the quality of the generative samples, and the failure to generate high-quality samples.

To solve this problem, this paper proposes an adaptive weight updating method, as shown in Figure 3. The method dynamically adjusts the weights of the gradient penalty term according to the loss of the discriminative network. Specifically, the update rule of the weight factor is based on the loss value of the discriminative network in each training step. When the loss of the discriminative network is large, it means that the model has not converged, and the weight of the gradient penalty term can be increased appropriately to enhance the constraints on the training of the model; while when the loss of the discriminative network is small, it means that the model tends to converge, and the weight factor can be reduced appropriately, so as to enable the generative network to learn more freely and avoid over-constraints.

This adaptive weight updating method can automatically adjust the penalty strength according to the actual situation during the training process, which improves the training efficiency of the model and can maintain the stability of the model throughout the training process, and ultimately generates more realistic and high-quality samples.

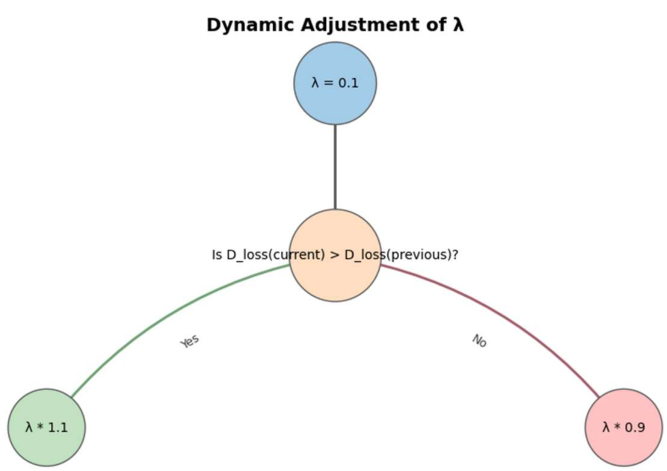

Fig. 3. Adaptive weight update

At the beginning of training, a small initial value (e.g., $\lambda_0 = 0.1$) is usually assigned to avoid premature overconstraint. Then, the weight factor λ is dynamically adjusted based on the loss changes in each round of training. The specific adjustment strategy is as follows:

If the loss of the current iteration increases compared to the previous one, it indicates that the generative network is underperforming and stronger constraints may be needed to facilitate training and prevent the quality of the generated data from deteriorating. Therefore, the weight of the gradient penalty can be increased and the update rule is: $\lambda \leftarrow 1.1\lambda$.

If the loss in the current iteration is reduced compared to the previous round, it means that the training of the generative network is progressing well, the current weights are performing appropriately, and the constraints no longer need to be overly enforced. Therefore, the weights of the gradient penalty can be reduced and the update rule is: $\lambda \leftarrow 0.9\lambda$.

The core idea of this dynamic adjustment strategy is to adjust the strength of the gradient penalty term in real time by observing the change of loss in each round of training, thus ensuring the flexibility of the training process. In this way, the constraints can be alleviated at the early stage of training so that the generative network has more degrees of freedom to learn, while at the later stage of training, the gradient penalty for the discriminative network is strengthened by increasing the weights to ensure that the generative network can ultimately generate high-quality samples, and to avoid the model from overfitting or collapsing.

This adaptive updating approach effectively improves the training stability of Generative Adversarial Networks (GANs) and accelerates the convergence process while enhancing the quality of the generated samples.

4. Modified LSTM prediction model

4.1. Model introduction

In order to improve the accuracy of gas concentration prediction, it has been shown that recurrent neural networks (RNNs) perform well in real-time gas prediction in longwall coal mines. RNNs influence the prediction at the current time step by utilizing the information from the previous time step, which is stored in the internal state of the RNN, thus enabling the use of dynamic context in the history of the input sequence. However, standard RNNs have a very limited range of context information accessible in practice, mainly due to their gradient vanishing problem. Specifically, the effects of the inputs on the hidden layer, and the contribution of these effects to the network output, fade or grow exponentially with recursive loops of time steps, resulting in a model that is unable to efficiently memorize long-term dependencies.

In a standard RNN, the state update of the hidden layer can be represented as:

$$h_t = \sigma\left(W_{hh}h_{t-1} + W_{xh}x_t + b_h\right) \tag{23}$$

where h_t denotes the hidden state at time step t, x_t is the input data, W_{hh} and W_{xh} are the weight matrices of the previous hidden state and the current input, respectively, b_h is the bias term, and σ is the activation function.

In the learning of long sequences, when the gradient is backpropagated, the gradient may gradually decay to close to zero, leading to the disappearance of the gradient, which in turn affects the training effect of the model. This is why the performance of standard RNNs in long sequence data is often unsatisfactory.

The Long Short-Term Memory (LSTM) network is a modified RNN designed to solve the problem of gradient vanishing. LSTM controls the transfer of information by introducing "cell states" and "gating mechanisms" that allow the information to remain constant over a long time span. The core structure of LSTM consists of three main gates. The core structure of LSTM consists of three main gates:

Forgetting Gate f_t: controls what information should be forgotten from memory. Its formula is:

$$f_t = \sigma\left(W_f \cdot \left[h_{t-1}, x_t\right] + b_f\right) \tag{24}$$

where f_t is the output of the forgetting gate, W_f is the weight matrix of the forgetting gate, $\left[h_{t-1}, x_t\right]$ is the splice of the hidden state of the previous time step and the current input, and b_f is the bias term.

Input Gate i_t: Controls which new information should be stored in the memory cell. Its formula is:

$$i_t = \sigma\left(W_i \cdot \left[h_{t-1}, x_t\right] + b_i\right) \tag{25}$$

where i_t is the output of the input gate, W_i is the weight matrix of the input gate, and b_i is the bias term.

Output Gate o_t: Controls how much information is output from the memory cell. The formula is:

$$o_t = \sigma\left(W_o \cdot \left[h_{t-1}, x_t\right] + b_o\right) \tag{26}$$

where o_t is the output of the output gate, W_o is the weight matrix of the output gate, and b_o is the bias term.

Memory unit c_t: Calculates the updated memory. Its formula is:

$$c_t = f_t \cdot c_{t-1} + i_t \cdot \tanh\left(W_c \cdot \left[h_{t-1}, x_t\right] + b_c\right) \tag{27}$$

where c_t is the state of the current memory cell, c_{t-1} is the state of the memory cell at the previous time step, W_c is the weight matrix associated with the current input memory update, b_c is the bias term, and $\tanh$ is the hyperbolic tangent activation function.

Final hidden state h_t: The final output state is:

$$h_t = o_t \cdot \tanh\left(c_t\right) \tag{28}$$

where h_t is the hidden state of the current time step.

Figure 4 shows the basic structure of LSTM.

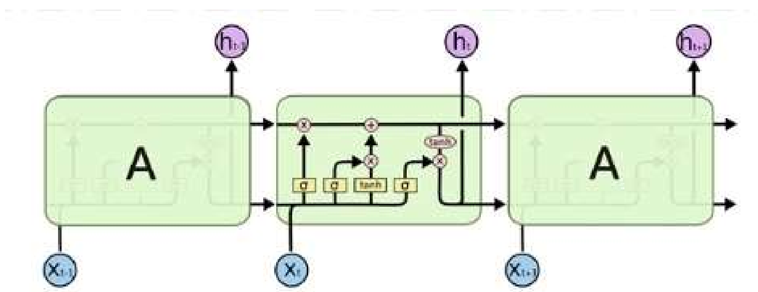

Fig. 4. LSTM basic structure diagram

The gating mechanism of LSTM allows the model to remember and use critical information over long time spans, avoiding the problem of gradient vanishing that exists in standard RNNs.

In this study, the LSTM network was modified to accommodate the task of predicting gas concentration. While standard LSTMs typically accept 2D data, this study modified it to use input shapes in 3D space. This included the addition of inputs related to spatial coordinates (x, y, z), as well as data related to the minimum distance from the coal miner, airflow velocity, and methane concentration, which were recorded at 1-second intervals. The modified LSTM model not only includes manipulation of 3D space, but also involves vector computation, further enhancing the model's capabilities in spatial prediction. The model predictions are shown in Figure 5.

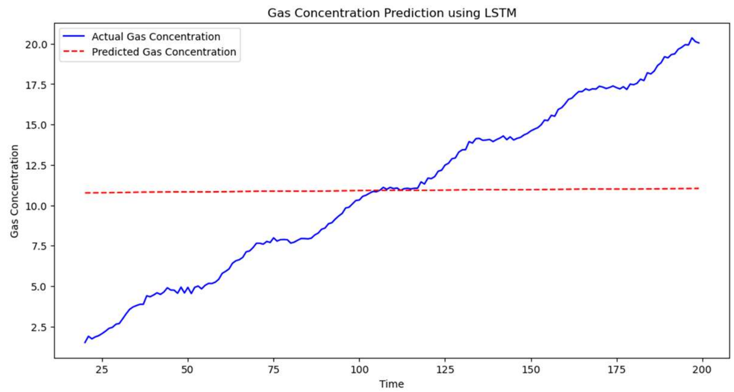

Fig. 5. LSTM model prediction results

Figure 6 illustrates the error at each moment, helping to analyze at which moments the model has large deviations.

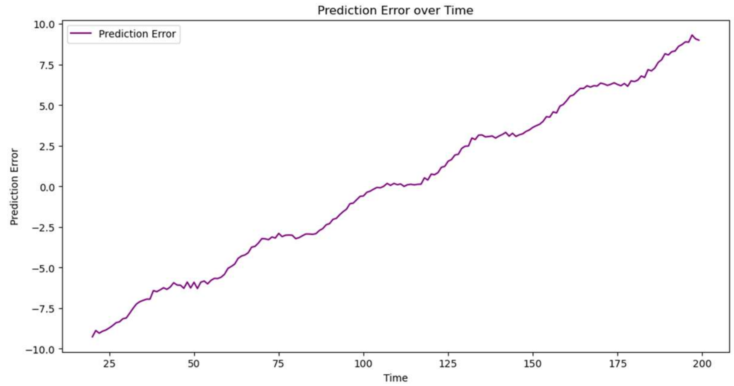

Fig. 6. Prediction error over time

Help assess whether the model has systematic errors by showing the residuals (the difference between the actual and predicted values), as shown in Figure 7.

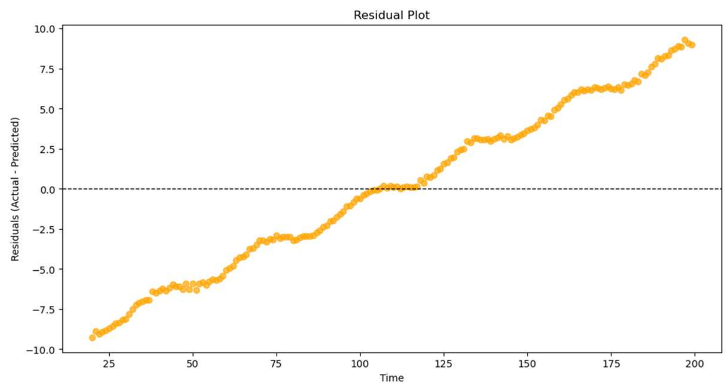

Fig. 7. Variance results

4.2. Model training

Repeated delivery of the same data is called an epoch, a simple explanation of an epoch is the complete delivery of the data set through the design network and the algorithm updates its parameters with each epoch as it learns the input data set. The training data for each instance was divided into 80% and 20% using a hierarchical K-folding cross-validation method, which produced a balanced division of the data that preserved the percentage methane content of each sample, and the divided 80% of the data was used to train the model.

4.3. Data validation

Training data and validation data are processed separately to evaluate the performance of the AI. The training and validation accuracies allow the user to evaluate the performance of the model. Figure 8 illustrates a commonly used metric for evaluating algorithm performance and shows the relationship between validation and training accuracies over epochs.

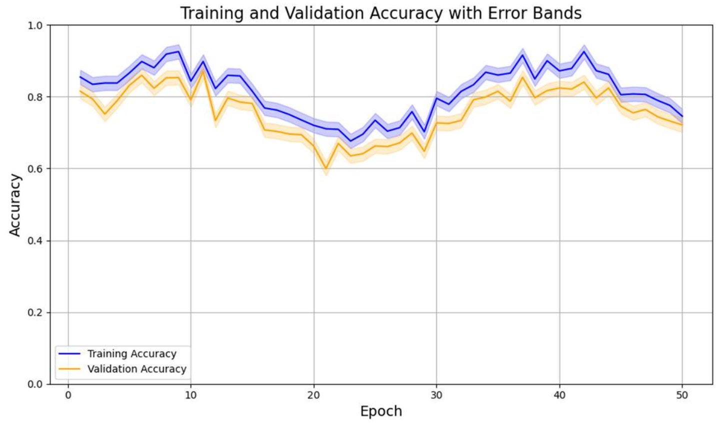

Fig. 8. Validation and Training Change Relationships

As can be seen from the graphs of training and validation accuracies, the slope of the curve flattens out after the 12th epoch, indicating that the data is no longer significant in learning the algorithm. From about the 20th epoch onwards, the learning curve becomes almost flat, which means that no further training is required after 20 epochs, as the accuracy does not change much, remaining between 89.1% and 93.8%. Finally, the validation curve lies below the training curve, indicating that the model represents the data well, is ready to be tested, and can provide reliable predictions.

With the improved LSTM model, combined with the characteristics of gas concentration prediction, this study is able to more accurately capture the long-term dependencies in the time series, solve the problem of gradient vanishing in the traditional RNN, and provide a more effective tool for real-time gas concentration prediction in coal mines.

5. Conclusion

This paper investigates the application of artificial intelligence technology in coal mine gas monitoring and prediction, and proposes an intelligent prediction model of gas concentration based on the combination of TCN-TimeGAN and improved LSTM to address the challenges faced by traditional monitoring methods in complex coal mine environments. The experimental results show that TCN-TimeGAN is able to effectively capture the time-dependent features and extreme fluctuations of gas concentration data by combining the interval sampling advantage of temporal convolutional networks and the adversarial training mechanism of generative adversarial networks, and realizes the accurate prediction of gas concentration in coal mines. And the improved LSTM network solves the problem of gradient vanishing in traditional RNNs by utilizing its gating mechanism, which further enhances the ability to capture long time-dependent features of time series. By introducing spatial data inputs, the improved LSTM not only can more accurately model the variation of gas concentration over time and space, but also provides a powerful tool for real-time gas monitoring.

In the model performance evaluation, TCN-TimeGAN and the improved LSTM show higher prediction accuracy and stability compared to traditional prediction methods. The experimental results show that the optimization strategy based on Wasserstein distance and gradient penalty effectively improves the training stability of the model and the quality of the generated data, and overcomes the gradient instability problem that occurs in the training of traditional generative adversarial networks. Meanwhile, combined with the hierarchical K-fold cross-validation method, the model proposed in this study shows high generalization ability and robustness on both the validation set and the training set, with prediction accuracies ranging from 89.1% to 93.8%, which demonstrates the reliability of the model.

In summary, the gas concentration prediction model based on TCN-TimeGAN and improved LSTM not only provides an intelligent and refined solution for gas monitoring in coal mines, but also provides a technical path that can be used for time-series data prediction in other fields. In future research, the model structure can be further optimized, and methods such as multidimensional data fusion and dynamic learning can be explored to improve the adaptability and real-time response ability of the model under extreme conditions, so as to provide a more perfect technical guarantee for the safe production of coal mines.

Funding

This research was supported by the Research on Multi-fan Combined Ventilation and Planning in Coal Mines, funded by the Key Research Project of Anhui Universities and Colleges (2022AH053157).

References

[1] Wei, L. J., Hu, J. K., Luo, X. R., & Liang, W. (2017). Study and analyze the development of China coal mine safety management. International Journal of Energy Sector Management, 11(1), 80-90.

[2] Li, X., Cao, Z., & Xu, Y. (2021). Characteristics and trends of coal mine safety development. Energy Sources, Part A: Recovery, Utilization, and Environmental Effects, 1-19.

[3] Ullah, M. F., Alamri, A. M., Mehmood, K., Akram, M. S., Rehman, F., Rehman, S. U., & Riaz, O. (2018). Coal mining trends, approaches, and safety hazards: a brief review. Arabian Journal of Geosciences, 11, 1-16.

[4] Yin, W., Fu, G., Yang, C., Jiang, Z., Zhu, K., & Gao, Y. (2017). Fatal gas explosion accidents on Chinese coal mines and the characteristics of unsafe behaviors: 2000–2014. Safety science, 92, 173-179.

[5] Zhu, Z., Wang, H., & Zhou, J. (2020). Monitoring and control model for coal mine gas and coal dust. Chemistry and Technology of Fuels and Oils, 56, 504-515.

[6] LI, Y., YANG, K., QIN, R., & YU, Y. (2020). Technical system and prospect of safe and efficient mining of coal and gas outburst coal seams. Coal Science and Technology, 48(3).

[7] Fu, G., Xie, X., Jia, Q., Tong, W., & Ge, Y. (2020). Accidents analysis and prevention of coal and gas outburst: Understanding human errors in accidents. Process safety and environmental protection, 134, 1-23.

[8] LIANG, Y., TIAN, F., FENG, W., SHAO, Z., MENG, X., & CHEN, C. (2021). Research progress of coal mine gas detection technology in China. Journal of China Coal Society, 46(6), 1701-1714.

[9] Chu, C., & Muradian, N. (2016). Safety and environmental implications of coal mining. International Journal of Environment and Pollution, 59(2-4), 250-268.

[10] Yuan, L. (2024). Progress and advancements of coal mine gas control and management for safe mining in China. Journal of Industrial Safety, 1(1), 100005.

[11] Jia, X., Shi, F., Guan, Y., Tang, S., & Tong, M. (2020, February). Zigbee-based wireless gas monitoring sensor alarm system in coal mine. In IOP Conference Series: Earth and Environmental Science (Vol. 446, No. 2, p. 022012). IOP Publishing.

[12] Jo, B. W., Khan, R. M. A., & Javaid, O. (2019). Arduino-based intelligent gases monitoring and information sharing Internet-of-Things system for underground coal mines. Journal of Ambient Intelligence and Smart Environments, 11(2), 183-194.

[13] Muduli, L., Mishra, D. P., & Jana, P. K. (2018). Application of wireless sensor network for environmental monitoring in underground coal mines: A systematic review. Journal of Network and Computer Applications, 106, 48-67.

[14] Deokar, S. R., & Wakode, J. S. (2017). Coal mine safety monitoring and alerting system. International

Research Journal of Engineering and Technology, 4(3), 2146-2149.

[15] Alfonso, I., Goméz, C., Garcés, K., & Chavarriaga, J. (2018, May). Lifetime optimization of Wireless Sensor Networks for gas monitoring in underground coal mining. In 2018 7th International Conference on Computers Communications and Control (ICCCC) (pp. 224-230). IEEE.

[16] Ali, M. H., Al-Azzawi, W. K., Jaber, M., Abd, S. K., Alkhayyat, A., & Rasool, Z. I. (2022). Improving coal mine safety with internet of things (IoT) based Dynamic Sensor Information Control System. Physics and Chemistry of the Earth, Parts a/B/C, 128, 103225.

[17] Chen, Y., Silvestri, L., Lei, X., & Ladouceur, F. (2022). Optically powered gas monitoring system using single-mode fibre for underground coal mines. International Journal of Coal Science & Technology, 9(1), 26.

[18] Chen, W., & Wang, X. (2020). Coal mine safety intelligent monitoring based on wireless sensor network. IEEE sensors journal, 21(22), 25465-25471.

[19] Liu, T., Wei, Y., Song, G., Hu, B., Li, L., Jin, G., ... & Wang, J. (2018). Fibre optic sensors for coal mine hazard detection. Measurement, 124, 211-223.

[20] Pudke, A. J., Bhagat, S. N., & Nalbalwar, S. L. (2017, June). LabVIEW based coal mine monitoring and alert system with data acquisition. In 2017 International Conference on Intelligent Computing and Control Systems (ICICCS) (pp. 1166-1170). IEEE.

[21] Xu, J., Yang, M., & Li, S. (2021). Hardware reliability analysis of a coal mine gas monitoring system based on fuzzy-FTA. Applied Sciences, 11(22), 10616.

[22] Demirkan, D. C., Duzgun, H. S., Juganda, A., Brune, J., & Bogin, G. (2022). Real-time methane prediction in underground longwall coal mining using AI. Energies, 15(17), 6486.

[23] Gong, W., Hu, J., Wang, Z., Wei, Y., Li, Y., Zhang, T., ... & Grattan, K. T. (2022). Recent advances in laser gas sensors for applications to safety monitoring in intelligent coal mines. Frontiers in Physics, 10, 1058475.

[24] Chen, P., Xie, Y., Jin, P., & Zhang, D. (2018). A wireless sensor data-based coal mine gas monitoring algorithm with least squares support vector machines optimized by swarm intelligence techniques. International Journal of Distributed Sensor Networks, 14(5), 1550147718777440.